

Model of Linear Quadratic Regulator (LQR) Control Method in Hovering State of Quadrotor

Oktaf Agni Dhewa^{1,2}, Andi Dharmawan², and Tri Kuntoro Priyambodo

¹Department Computer Science and Electronics

²Aerospace and Satellite Group Research

Oktaf.ad@mail.ugm.ac.id

Abstract— Quadrotor is an unmanned aircraft which has vertical take-off and landing (VTOL) capability. However quadrotor requires a good control system to itself during flight. So, the aim of this research is to design and implement a control system on quadrotor using LQR method to obtain the best feedback gain K value in hover state. LQR is a method that calculates the optimal feedback gain K . The feedback gain K can be determined by tuning of Q and R . The feedback gain is used to control the system in control signal form. The control signal values are converted into PWM to control brushless motor speed to maintain quadrotor's position. The test results show, Q and R values of the same roll and pitch were $Q = 0.08$ and $R = 1$, where the average angle of roll of 0.25 degrees and the average angle of pitch of 0.15 degrees. While the value of Q and R yaw angles were $Q = 0.01$ and $R = 1$, the yaw angle maintains in the range of an angle of 0 degrees to 2 degrees. As for the rise time, roll angle was able to handle distractions for 0.09 seconds, 0.15 seconds during the pitch angle and 0.12 seconds during the yaw angle.

Index Terms— Optimal Control; Orientation Angles; Hovering.

I. INTRODUCTION

UAV (Uninhabited Aerial Vehicle or Unmanned Aerial Vehicle) is known as unmanned aircraft which uses aerodynamic forces to fly [9]. UAVs is capable of flying autonomously (autonomous), so it does not require the pilot to fly it. UAVs can be controlled from a long distance using a remote control and can carry payload [2].

UAV has been developed and used for various purposes. At this time, UAV is not only developed on military missions, but also UAV is being developed to help civilian missions like aerial surveillance, reconnaissance, inspection on a complex and dangerous environments, aerial photography, transportation of goods, and much more [1][10].

Panoramic photo, capturing images of natural disasters, are some applications of aerial photography missions that require stable condition at a certain height to get a picture with good results. In addition UAV is required to be able to fly with limited space if the shooting area is obstacles and difficult to reach.

One type of UAV with that ability is a quadrotor. Quadrotor is among of the drones often called UAV that can take-off and landing vertically even in a limited area [2]. Quadrotor can also hover in a particular area is supporting the mission of aerial photographs. However, quadrotor requires a good control system to maintain its stability during flight. Because in the absence of that, quadrotor will be difficult to be controlled.

There are various methods of control systems. One of the control methods is LQR (Linear Quadratic Regulator). This control is an optimal control that has robust characteristics with regulator property and it produces a steady state minimum error [4]. This method can also to resolve errors that occur in the system quickly. So, the system can maintain stability to environmental disturbance,

The aim of this research is to design and implement a control system on quadrotor using LQR method to obtain feedback gain K value while quadrotor in hover state. The best value of feedback gain K can be determined by tuning the values of Q and R based on real test flight experiment results rather than simulation.

II. QUADROTOR DYNAMICS

A. Dynamics Model of Quadrotor

Quadrotor has six degrees of freedom (DOF) which are described by the two reference frames. These frames are an earth inertial reference (E-frame) and body fixed reference (B-frame) [3]. The illustration of B-frame to E-frame is given in Figure 1.

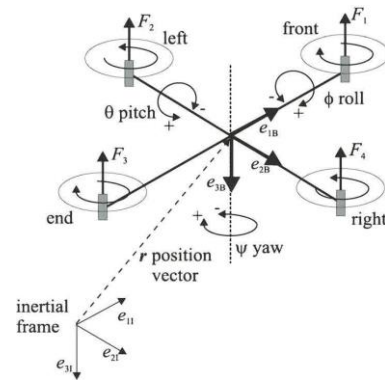


Figure 1: The illustration of B-frame to E-frame [3]

The dynamic model is derived using Newton-Euler formalism as shown in [18]. The dynamics of a rigid body under external forces applied to the center of mass and expressed in the body-fixed frame are formulated in Equation 1 as shown in [20],

$$\begin{bmatrix} m_{3 \times 3} & 0 \\ 0 & I \end{bmatrix} \begin{bmatrix} V \\ \dot{\omega} \end{bmatrix} + \begin{bmatrix} \omega \times (mV) \\ \omega \times (I\omega) \end{bmatrix} = \begin{bmatrix} F \\ \tau \end{bmatrix} \quad (1)$$

where $I \in \mathcal{R}^{3 \times 3}$ is the inertia matrix, V is the body linear speed vector and ω is the body angular speed. The

equations of motion for the quadrotor can be written as in [19],

$$\begin{cases} \zeta = v \\ m\dot{v} = RF_b \\ \dot{R} = R\hat{w} \\ J\dot{w} = -w.Jw + \tau_a \end{cases} \quad (2)$$

The first-level approximate model (3) of the Quadrotor can be rewritten as [16],

$$\begin{cases} \zeta = v \\ \dot{v} = -ge_3 + R_e 3(\frac{b}{m} \sum \Omega_i^2) \\ \dot{R} = R\hat{w} \\ I\dot{w} = -wIw - \sum J_\tau (we_3)\Omega_i + \tau_a \end{cases} \quad (3)$$

The torque applied on the vehicle's body along an axis is the difference between the torque generated by each propeller on the other axis.

$$\tau_a = \begin{pmatrix} lb(\Omega_4^2 - \Omega_2^2) \\ lb(\Omega_3^2 + \Omega_1^2) \\ d(\Omega_2^2 + \Omega_4^2 - \Omega_1^2 - \Omega_3^2) \end{pmatrix} \quad (4)$$

the rotor (propulsion group) inertia is then [16]

$$J_r = J_p - J_m r \quad (5)$$

The full dynamic model of quadrotor can be shown in equation (6) to (11) [16]

$$\ddot{x} = (\cos \phi \sin \theta \cos \psi + \sin \phi \sin \psi) \frac{F}{m} \quad (6)$$

$$\ddot{y} = (\cos \phi \sin \theta \sin \psi - \sin \phi \cos \psi) \frac{F}{m} \quad (7)$$

$$\ddot{z} = -g + (\cos \phi \cos \theta) \frac{F}{m} \quad (8)$$

$$\dot{p} = \frac{I_{yy} - I_{zz}}{I_{xx}} qr - \frac{J_r}{I_{xx}} q\Omega + \frac{u_2}{I_{xx}} \quad (9)$$

$$\dot{q} = \frac{I_{zz} - I_{xx}}{I_{yy}} pr - \frac{J_r}{I_{yy}} p\Omega + \frac{u_3}{I_{yy}} \quad (10)$$

$$\dot{r} = \frac{I_{xx} - I_{yy}}{I_{zz}} pq + \frac{u_4}{I_{zz}} \quad (11)$$

B. State Space Model of Quadrotor

The state model can be obtained from the linearization of dynamic model of quadrotor. It can be shown in equation (12) [14].

$$\begin{bmatrix} \dot{x} \\ \dot{y} \\ \dot{z} \\ V_x \\ V_y \\ V_z \\ \phi \\ \theta \\ \psi \\ p \\ q \\ r \end{bmatrix} = \begin{bmatrix} 0 & 0 & 0 & 1 & 0 & 0 & 0 & 0 & 0 & 0 & 0 & 0 \\ 0 & 0 & 0 & 0 & 1 & 0 & 0 & 0 & 0 & 0 & 0 & 0 \\ 0 & 0 & 0 & 0 & 0 & 1 & 0 & 0 & 0 & 0 & 0 & 0 \\ 0 & 0 & 0 & 0 & 0 & 0 & 0 & \frac{u_1}{m} & 0 & 0 & 0 & 0 \\ 0 & 0 & 0 & 0 & 0 & 0 & -\frac{u_1}{m} & 0 & 0 & 0 & 0 & 0 \\ 0 & 0 & 0 & 0 & 0 & 0 & 0 & 0 & 0 & 0 & 0 & 0 \\ 0 & 0 & 0 & 0 & 0 & 0 & 0 & 0 & 0 & 1 & 0 & 0 \\ 0 & 0 & 0 & 0 & 0 & 0 & 0 & 0 & 0 & 0 & 1 & 0 \\ 0 & 0 & 0 & 0 & 0 & 0 & 0 & 0 & 0 & 0 & 0 & 1 \\ 0 & 0 & 0 & 0 & 0 & 0 & 0 & 0 & 0 & 0 & 0 & 0 \\ 0 & 0 & 0 & 0 & 0 & 0 & 0 & 0 & 0 & 0 & 0 & 0 \\ 0 & 0 & 0 & 0 & 0 & 0 & 0 & 0 & 0 & 0 & 0 & 0 \end{bmatrix} \begin{bmatrix} x \\ y \\ z \\ V_x \\ V_y \\ V_z \\ \phi \\ \theta \\ \psi \\ p \\ q \\ r \end{bmatrix} + \begin{bmatrix} 0 & 0 & 0 & 0 \\ 0 & 0 & 0 & 0 \\ 0 & 0 & 0 & 0 \\ 0 & 0 & 0 & 0 \\ \frac{1}{m} & 0 & 0 & 0 \\ 0 & 0 & 0 & 0 \\ 0 & 0 & 0 & 0 \\ 0 & \frac{1}{I_{xx}} & 0 & 0 \\ 0 & 0 & \frac{1}{I_{yy}} & 0 \\ 0 & 0 & 0 & \frac{1}{I_{zz}} \end{bmatrix} \begin{bmatrix} u_1 \\ u_2 \\ u_3 \\ u_4 \end{bmatrix} \quad (12)$$

III. CONTROL SYSTEM

A. Linear Quadratic Regulator (LQR) Control

LQR is an optimal control that has a robust and produces a steady state minimum error [4]. The simulated block diagrams of state feedback controller displayed in Figure 2.

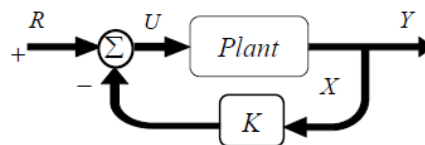


Figure 2: Block diagram of LQR controller [5]

In LQR, a cost function is minimized to provide the best control signal. A cost function is formulated in equation (13).

$$J = \int_{t^0}^{\infty} (\mathbf{x}^T \mathbf{Q} \mathbf{x} + \mathbf{u}^T \mathbf{R} \mathbf{u}) dt \quad (13)$$

Refers to the equation (13), LQR control is determined by the Q and R metrics. Selection of appropriate Q and R values will be obtained the best feedback gain values for plant system. The feedback gain can calculated by the derived equation from equation (13) using Hamilton-Jacobi-Bellman method. The equation can be solved by algebraic Ricatti equation (ARE), that can be shown in equation (14).

$$\mathbf{A}^T \mathbf{S} + \mathbf{S} \mathbf{A} - \mathbf{S} \mathbf{B} \mathbf{R}^{-1} \mathbf{B}^T \mathbf{S} + \mathbf{Q} = \mathbf{0} \quad (14)$$

S is auxiliary variable to determine feedback gain K.

Control signal is result from multiple values between negative feedback gain K and state control as in the equation (15).

$$\mathbf{u} = -\mathbf{K} \mathbf{x} \quad (15)$$

So, the feedback gain K can be written in equation (16)

$$\mathbf{K} = \mathbf{R}^{-1} \mathbf{B}^T \mathbf{S} \quad (16)$$

The selection matrices Q and R are as follow:

- The larger weight matrices Q will increase the value of gain feedback (K) which can make fast response system to achieve intermediate state cost function.
- The larger weight matrices R will decrease the value of gain feedback (K) which can slow down steady state (energy drive).

B. LQR Control Design of Quadrotor for Hovering State

In the equation of state models, there are 12 states of quadrotor can be controlled. However, the basic principle of hover is the control of quadrotor rotation motion. The rotation states controlled is interpreted six state, i.e., ϕ , θ , ψ , p , q , and r representing the roll, pitch, and yaw, so that the states equation model (12) can be shown in equation (17).

$$\begin{bmatrix} \dot{\phi} \\ \dot{\theta} \\ \dot{\psi} \\ \dot{p} \\ \dot{q} \\ \dot{r} \end{bmatrix} = \begin{bmatrix} 0 & 0 & 0 & 1 & 0 & 0 \\ 0 & 0 & 0 & 0 & 1 & 0 \\ 0 & 0 & 0 & 0 & 0 & 1 \\ 0 & 0 & 0 & 0 & 0 & 0 \\ 0 & 0 & 0 & 0 & 0 & 0 \\ 0 & 0 & 0 & 0 & 0 & 0 \end{bmatrix} \begin{bmatrix} \phi \\ \theta \\ \psi \\ p \\ q \\ r \end{bmatrix} + \begin{bmatrix} \frac{1}{I_{xx}} \\ 0 \\ 0 \\ 0 \\ \frac{1}{I_{yy}} \\ 0 \\ 0 \\ 0 \\ \frac{1}{I_{zz}} \end{bmatrix} \begin{bmatrix} u_2 \\ u_3 \\ u_4 \end{bmatrix} \quad (17)$$

The component of control signal u_1 is not controlled.

This is due to an signal process u_1 in form of thrust altitude, which is handled by throttle from remote.

The moment of inertia for axis x , y and z can be calculated using the equation has been developed. The moment of inertia shown in equation (18) to (19) [12].

$$I_{xx} = \frac{mr^2}{4} + \frac{mh^2}{6} + 2mr^2 + \frac{MR^2}{4} + \frac{MH^2}{12} \quad (18)$$

$$I_{yy} = \frac{mr^2}{4} + \frac{mh^2}{6} + 2mr^2 + \frac{MR^2}{4} + \frac{MH^2}{12} \quad (19)$$

$$I_{zz} = 4mr^2 + \frac{MR^2}{2} \quad (20)$$

Equations are applied in Figure 3. Components of I_{xx} , I_{yy} , and I_{zz} are part of the inertia equation.

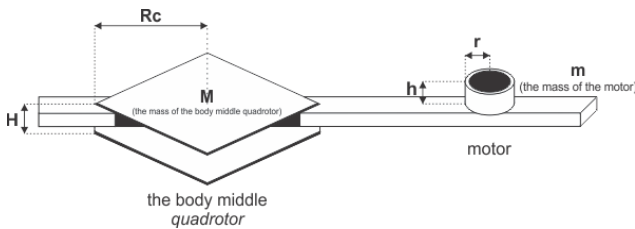


Figure 3. Inertia equation x , y , z

where component H is the height of the CM (Center of Mass), Rc is the radius of middle body quadrotor, M is the mass of the middle body quadrotor, h is the height of the motor, r is the radius of the motor, and m is the mass of the motor.

Moreover, every states controlled can be obtained from IMU sensor readings using Madgwick quaternion fusion method and Kalman filter to get more accurate data. This fusion produces roll angle (θ), pitch angle (ϕ) and the angular velocity x , y , and z , while yaw angle (ψ) is produced by compass sensor.

Control signal (\mathbf{u}) can be obtained by calculating with reference to the equation (15). So the equation linearity

control signal of a system, which will be given to the motor, can be expressed as following,

$$u_2 = K_{00} * \text{roll_degree} + K_{03} * \text{angular_velocity_x} \quad (21)$$

$$u_3 = K_{11} * \text{pitch_degree} + K_{14} * \text{angular_velocity_y} \quad (22)$$

$$u_4 = K_{44} * \text{yaw_degree} + K_{25} * \text{angular_velocity_z} \quad (23)$$

where u_2 is control signal for *roll*, u_3 is control signal for *pitch* and u_4 is control signal for *yaw*.

Not only the calculation applied to the motor but also analysis of the position of laying the IMU sensor (accelerometer and gyroscope) in determining the thrust and torque quadrotor is required. This study uses a type quadrotor with a plus (+) which can represented motor position in the front, right, rear and left on frame of quadrotor.

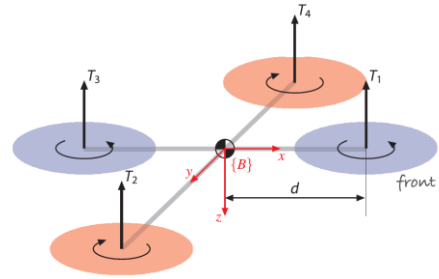


Figure 4. Quadrotor type + [6]

Figure 4 refers to the body-fixed frame (B) and is the center of mass of the quadrotor. Motor 1 and 3 is a motor to move the quadrotor toward the front and back. This motors rotate counter-clockwise. Motor 2 and 4 is a motor to move the quadrotor toward the right and left, that rotate clockwise.

The sign of pitch and roll angle is determined from imu sensor position. The value of pitch angle has a positive value, if the motor 1 position higher than the motor 3 and vice versa, while the value of the roll angle has a positive value, if the motor 4 position higher than motor 2 and vice versa.

The direction rotation of the propeller and the position of IMU make thrust of quadrotor with equation (24) [7].

$$T_i = b\omega^2, i=1,2,3,4 \quad (24)$$

where i is the i -th motor. Quadrotor translational motion is shown in equation (25).

$$m\dot{v} = \begin{pmatrix} 0 \\ 0 \\ mg \end{pmatrix} - {}^0R_B \begin{pmatrix} 0 \\ 0 \\ T \end{pmatrix} \quad (25)$$

where m is the mass of quadrotor, \dot{v} is the first derivative of velocity, T is the total thrust, and 0R_B is the coordinate frame of the earth. Torque x -axis quadrotor which is rolling torque shown in equation (26) and (27).

$$\tau_x = dT_4 - dT_2 \quad (26)$$

$$\tau_x = db(\omega_4^2 - \omega_2^2) \quad (27)$$

where d is the radius measured from the midpoint of the center of mass to the midpoint of the motor.

Torque y-axis is pitching torque can be elaborated in equation (28) and (29).

$$\tau_y = dT_1 - dT_3 \quad (28)$$

$$\tau_y = db(\omega_1^2 - \omega_3^2) \quad (29)$$

The torque applied to each vane by motorcycle against the frictional force of air can be obtained by equation (30).

$$Q_i = k\omega_i^2 \quad (30)$$

where k is a factor such as b, then the total torque reaction of the z-axis described by equation (31) and (32).

$$\tau_z = Q_1 - Q_2 + Q_3 - Q_4 \quad (31)$$

$$\tau_z = k(\omega_1^2 + \omega_3^2 - \omega_2^2 - \omega_4^2) \quad (32)$$

Yaw torque can be controlled by using the estimated coordinates of the four motors. Based on Euler equations for a rotating movement of quadrotor the yaw axis has the equation (33).

$$\mathbf{J}\dot{\bar{\omega}} = -\bar{\omega}\mathbf{J}\bar{\omega} + \mathbf{\Gamma} \quad (33)$$

where \mathbf{J} is 3 x 3 inertia matrix of quadrotor, $\bar{\omega}$ is the angular velocity vector, dan $\mathbf{\Gamma} = (\tau_x, \tau_y, \tau_z)^T$ is the torque of quadrotor. The motion of quadrtoor can obtained from the integration of the dynamic equations of equation (21) and (28), in which the forces and moments on quadrotor style can be seen in equation (34).

$$\begin{pmatrix} \mathbf{T} \\ \mathbf{\Gamma} \end{pmatrix} = \begin{pmatrix} -b & -b & -b & -b \\ 0 & -db & 0 & db \\ db & 0 & -db & 0 \\ k & -k & k & -k \end{pmatrix} \begin{pmatrix} \omega_1^2 \\ \omega_2^2 \\ \omega_3^2 \\ \omega_4^2 \end{pmatrix} = \mathbf{A} \begin{pmatrix} \omega_1^2 \\ \omega_2^2 \\ \omega_3^2 \\ \omega_4^2 \end{pmatrix} \quad (34)$$

So the function of the motor speed is described in equation (35).

$$\begin{pmatrix} \omega_1^2 \\ \omega_2^2 \\ \omega_3^2 \\ \omega_4^2 \end{pmatrix} = \mathbf{A}^{-1} \begin{pmatrix} T \\ \tau_x \\ \tau_y \\ \tau_z \end{pmatrix} \quad (35)$$

Control of each motor using LQR control can obtained from equation (35) with T is not controlled. So, the -b components not included in each torque of quadrotor. The torque x, y, and z are the signal control of equation (21) to (23) [6]. The angular velocity function of each motor can calculated by equation (36).

$$\begin{pmatrix} \omega_1^2 \\ \omega_2^2 \\ \omega_3^2 \\ \omega_4^2 \end{pmatrix} = \left(\frac{1}{\det \mathbf{A}} \right) \begin{pmatrix} 0 & 0 & db & k \\ 0 & -db & 0 & -k \\ 0 & 0 & -db & k \\ 0 & db & 0 & -k \end{pmatrix} \begin{pmatrix} u_1 \\ u_2 \\ u_3 \\ u_4 \end{pmatrix} \quad (36)$$

So the pulse which is given to the control of each motor in the equation (37) to (40).

$$front_motor = \left(\frac{1}{\det \mathbf{A}} \right) (u_3 * db + u_4 * k) \quad (37)$$

$$right_motor = \left(\frac{1}{\det \mathbf{A}} \right) (u_2 * -db + u_4 * -k) \quad (38)$$

$$rear_motor = \left(\frac{1}{\det \mathbf{A}} \right) (u_3 * -db + u_4 * k) \quad (39)$$

$$left_motor = \left(\frac{1}{\det \mathbf{A}} \right) (u_2 * db + u_4 * -k) \quad (40)$$

In searching constants b and k can be obtained from the equation (41) and (42) which are thrust and torque [17].

$$T = C_T \rho A R^2 \omega^2 \quad (41)$$

$$Q = C_Q \rho A R^3 \omega^2 \quad (42)$$

Based on equation (24) and (25), the constant b = $C_T \rho A R^2$ and the constant k = $C_Q \rho A R^3$, where T is thrust, Q is the torque, C_T and C_Q is thrust dimensionless coefficient and torque, ρ is the density of air (1,184 kg / m³), A is the area blade when rotating ($2\pi^2$), R is the radius of blade (rps) [17].

IV. ARCHITECTURE SYSTEMS

A. Architecture and Electronic System

The electronic system of quadrotor utilizes IMU sensor that consists of 3 DOF accelerometer and 3 DOF gyroscope used for reading acceleration and the angular velocity in the each axis x, y, z. Compass sensor is used for reading yaw angle. In additional, the motor brushless is used as an actuator of the system. The motor are controlled with ESC (Electronic Speed Controller). The microcontroller used in this research is ARM cortex M4.

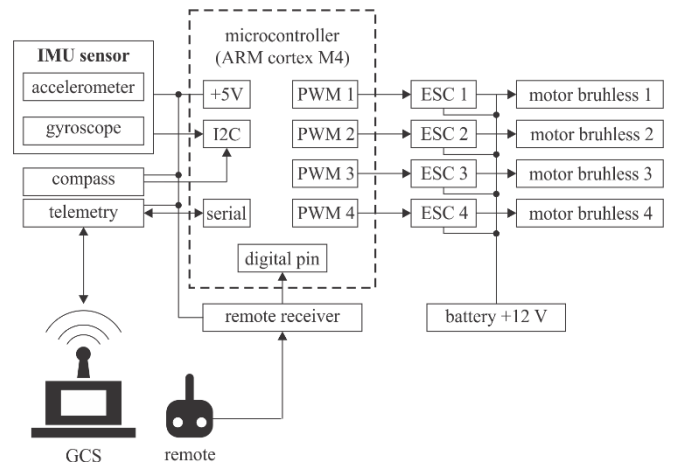


Figure 5: Architecture system of quadrotor

The accelerometer, gyroscope and compass sensors communicate with microcontroller using I2C data lines are SDA (Serial Data) and SCL (Serial Clock) and digital pin interrupt as the data sender. The output of the IMU sensor is

an angle to the axis x, y, and z. The value is compared with the angle of desired value (the desired angle). Results of the comparison are converted into a pulse value through pin PWM (Pulse Width Modulation) of microcontroller. The pulse of PWM will be given to a brushless motor controlled by the ESC. Besides of that, the thrust of quadrotor is handled by signal throttle from remote, that the signal is received on microcontroller using receiver module through digital pin interrupt.

All quadrotor data read by sensor will be transmitted to the ground control station using telemetry module 433 MHz. The telemetry communicated with microcontroller using serial communication. The telemetry module get the supply of the microcontroller pin out by 5 Volt as well as for all sensors and remote receiver, while the microcontroller and the ESC get supply voltage of battery 12 volts with a current 2200 mAh.

B. Draft Control System

As in the system architecture, system analysis concerning the previous section, so in the control system quadrotor as a whole because this research is focus on the control system. The control which is used in this system is LQR control system. LQR control system is an optimal control system which is implemented in the form of space and time (state space).

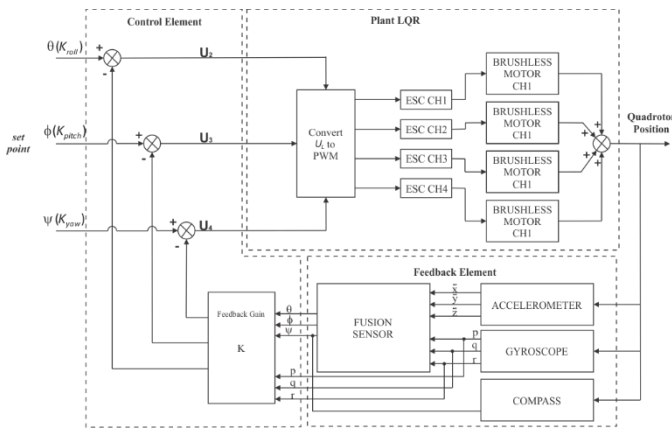


Figure 6 : LQR control diagram of quadrotor

Figure 6 explains that the system control signal derived from IMU sensor (accelerometer and gyroscope) with the output angle and angular velocity to the axis x (p), y (q), and z (r). Data from IMU sensor will be converted into a roll angle (x-axis) and pitch (y-axis) through fusion sensor (Madgwick quaternion and Kalman filter), while yaw angle (z-axis) can be obtained from compass sensor.

Roll angle, pitch angle, yaw angle and angular velocity p, q, r, which are generated, are regarded as state of the system, by multiplying the negative full state feedback gain as LQR control which will be the signal control of process system. Next, the input system will be compared to the desired value, wherein the desired value in this study is the angle of 0 ° for each orientation angle. Difference between value from sensor and desired value will be converted to PWM signal and then the signal are given to the plant system.

C. Software Design

Designing software is used to an algorithm for accessing the sensors, actuators, and other devices in the quadrotor

system. The algorithm is built using the C ++ programming language.

The function of main program is shown in Figure 7. This function is intended for quadrotor to be able to fly and hover easily.

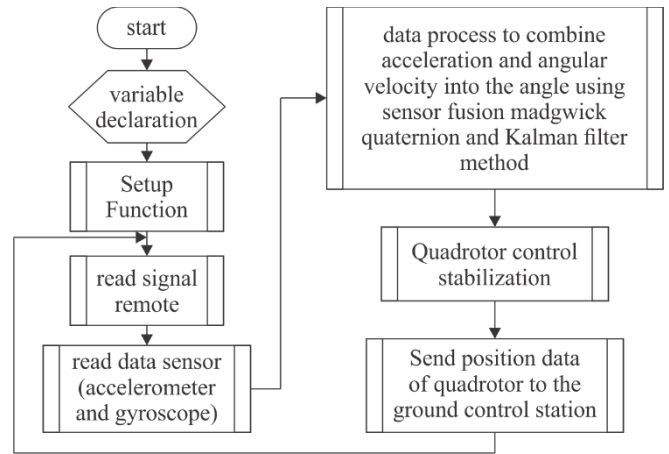


Figure 7: Flowchart of quadrotor main program

D. Mechanical Design of Quadrotor

Quadrotor mechanics are built by utilizing aluminium as a quadrotor arm material and acrylic as a quadrotor body material.

On the part of the quadrotor body is divided into 2 parts space. First part in the lower level of the shield laying quadrotor used only supply voltage of 12 Volt batteries, while second part in the upper level is used to put the electronic parts, sensors, remote receiver and telemetry modules.

The size of quadrotor is clearly shown in Figure 8.

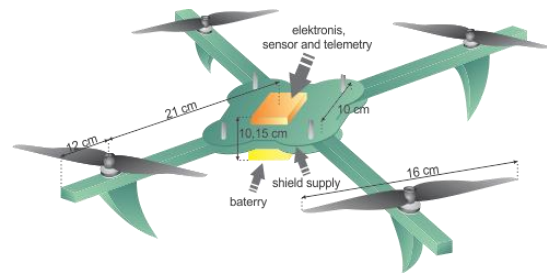


Figure 8: Mechanical design of quadrotor

Implementation of mechanical design of quadrotor is depicted in below Figure 9.



Figure 9: Implementation of the quadrotor mechanical design

E. Parameters of Quadrotor

All parameters of LQR control system of quadrotor shown in Table 1.

Table 1
Parameters of Quadrotor

Parameter	Value	Unit
M	4.25×10^{-1}	kg
R_c	0.79×10^{-1}	meter
H	10.15×10^{-2}	meter
m	0.25×10^{-1}	kg
r	0.14×10^{-1}	meter
h	0.16×10^{-1}	meter
C_T	0.05×10^{-1}	
C_Q	2.28×10^{-1}	
R	0.21	meter
ρ	11.84×10^{-1}	kg.m ⁻³
A	13.85×10^{-2}	m
I_{xx}	1.04×10^{-3}	
I_{yy}	1.04×10^{-3}	
I_{zz}	1.35×10^{-2}	
b	36.15×10^{-6}	
k	34.62×10^{-8}	

V. RESULT AND ANALYSIS

A. Brushless Motor Test

Each motor have its own character though with the same type, therefore it is necessary to test the motor to get its characteristics

The first test was applied to determine pulse width dead zone in motor. This test is performed to find the starting point of each motor in a spin. The greater the value of the starting point will make the motor rotates more slowly than the other motor for the same pulse. Based on experiments is obtained pulse width dead zone for each motor as shown in Table 2.

Table 2
Dead Zone Each Motor

Motor	Pulse width dead zone
Front Motor	1107
Right Motor	1106
Left Motor	1087
Rear Motor	1106

Dead zone is the minimum voltage required by the propeller to rotate or revolve [13]. As seen in Table 1, the pulse width dead zone that has the widest pulse width is the front motor and the smallest pulse is the rear motor, so logically the motor with a smaller pulse width dead zone will have faster speeds than other motors. But according to experimental data, it is known that rotating speed of the motor with the same pulse width dead zone does not necessarily have the same speed. This is shown in Table 3 which displays data about the speed of the motor.

Table 3
Motor Brushless Data

PWM	1200	1400	1500	1600	1700
Fm	296.93	455.30	536.83	599.84	662.54
Rm	299.76	526.57	592.20	661.70	694.99
Lm	352.20	561.54	634.70	703.67	750.04
Rrm	306.88	535.37	590.84	670.08	704.30

where PWM in (micro seconds), Fm is Front motor (rad/s), Rm is Right motor (rad/s), Lm is Left motor (rad/s), and Rrm is Rear motor (rad/s).

So it needs a motor speed linearity to get the same thrust lift on the pulse change [11].

The Linearization of the pulse and motor speed for each brushless motor based on data Table 2. The linearization chart is shown in Figure 10.

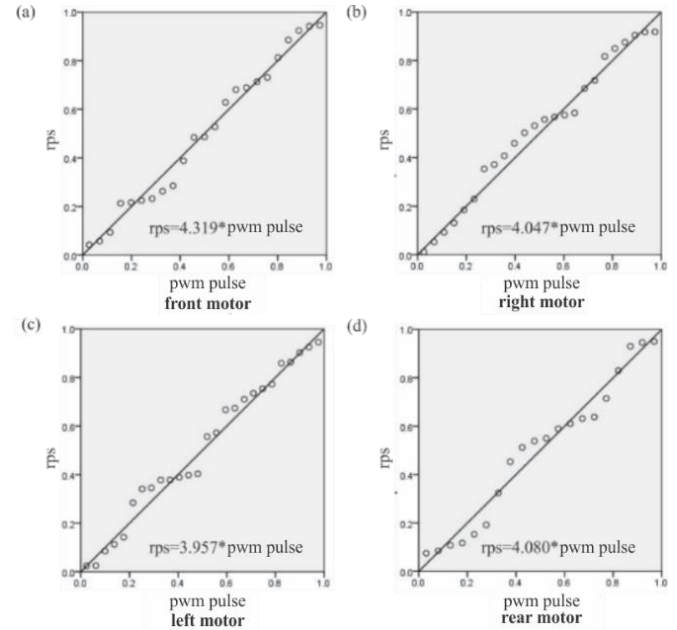


Figure 10. Linearization chart from motor brushless data

Linear equations, which are formed. are $y = mx$, where y represents the value of the motor speed (rps) and x represents the value of PWM pulse width. The constant values of each motor are 4.319 for Figure 10 (a), 4,047 to Figure 10 (b), 3957 to Figure 10 (c), and 4,080 to Figure 10 (d).

The application of algorithm program that is inserted into the microcontroller, the rps value is represented by variable w_0 . So, pulse's value of brushless motor can be written in equation (43)

$$Pulse_motor_i(1,2,3,4) = ((w_0 + wc) / m) + deadzone + throttle \quad (43)$$

where wc is the calculation of LQR control and m is constants linearity. The approach of the right different pulse for each motor, then each motor has the same lift.

B. LQR Control Test

Roll angle, pitch, and yaw testing with different weighting of Q and R

Roll angle Testing

The variations of Q value for roll angle testing are shown in Table 4.

Table 4
Variations of Q Value in Roll Angle

Q	R	K
0.00001 0 0 0 0 0 0 0 0 1 0 0	1	0.000031 0 0 0.002469 0 0
0.05 0 0 0 0 0 0 0 0 1 0 0	1	0.002236 0 0 0.020737 0 0
0.075 0 0 0 0 0 0 0 0 1 0 0	1	0.002739 0 0 0.022949 0 0
0.08 0 0 0 0 0 0 0 0 1 0 0	1	0.002828 0 0 0.023322 0 0
0.085 0 0 0 0 0 0 0 0 1 0 0	1	0.002915 0 0 0.0236787 0 0

The value of feedback gain K will be even greater if the Q value also increases. This is occur, because Q value is directly proportional to the value of Riccati (S) calculation result. Results variations in Q and R values based on Table 4 are shown in Figure 11.

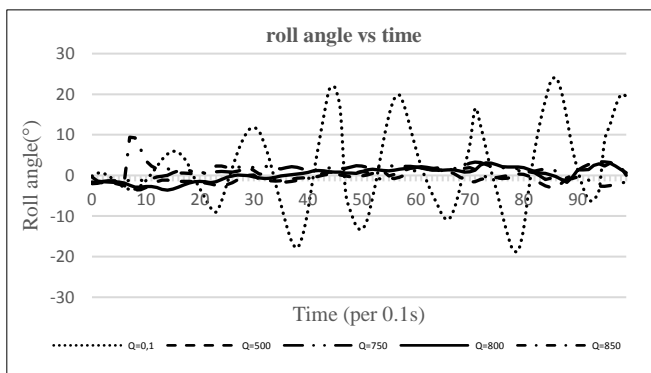


Figure 11. Graph of roll angle versus time with variations in Q value

The system had experienced oscillation when it was given a small Q value which was 0.00001 and the R value of 1. A small Q value will produces the gain of a small K value as well. The K value will affect the value input system which is proportional to the control signal system [15].

A small input system will produce a small output value and it will lead to changes in a small PWM value, so that the speed of response system becomes long in achieving stability. Variation in weighting Q and R for best quadrotor roll angle within 10 seconds that is $Q = 0.08$ and $R = 1$ with a roll angle obtained an average of $0,25^\circ$ and a standard deviation of $1,69^\circ$.

Pitch angle testing

Based on experimental flight with the variation Q values 0.00001, 0.05, 0.055, 0.08 and 0.085 is obtained result as shown in Figure 12.

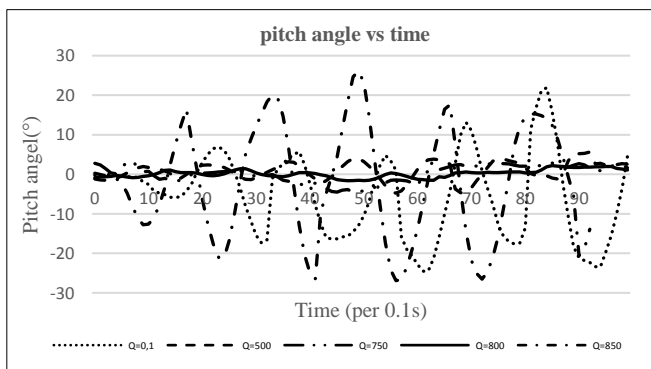


Figure 12. Graph of pitch angle versus time with the variation of Q value

The value of 0° which occurs in provision of the value $Q = 0.075$ and $Q = 0.08$. However, the standard deviation of pitch angle value that has minimum errors contained in the Q value of 0.08, so the selected Q is $Q = 0.08$ and $R = 1$ with an average angle of 0.15° and a standard deviation of 1.01° . In addition to Q value of 0.08 has a faster response speed in reaching a steady state than Q value of 0.075. So, the Q value of 0.08 is the best value which is required by this system. The system has better robust properties and minimum errors in a steady state compared to the weighting of Q of 0.085 or 0.075.

Yaw angle testing

Based on many experiments, five best data with values Q and R are shown in Table 5.

Table 5
Variations of Q Value in Yaw Angle

Q	R	K
0 0 0.00001 0 0 0 0 0 0 0 0 1	1	0 0 0.000031 0 0 0.002169
0 0 0 0.05 0 0 0 0 0 0 0 1	1	0 0 0.002236 0 0 0.018228
0 0 0 0.055 0 0 0 0 0 0 0 1	1	0 0 0.002345 0 0 0.018768
0 0 0 0.08 0 0 0 0 0 0 0 1	1	0 0 0.002828 0 0 0.020501
0 0 0 0.1 0 0 0 0 0 0 0 1	1	0 0 0.003163 0 0 0.021676

Implementing in the form of a graph as shown in Figure 13.

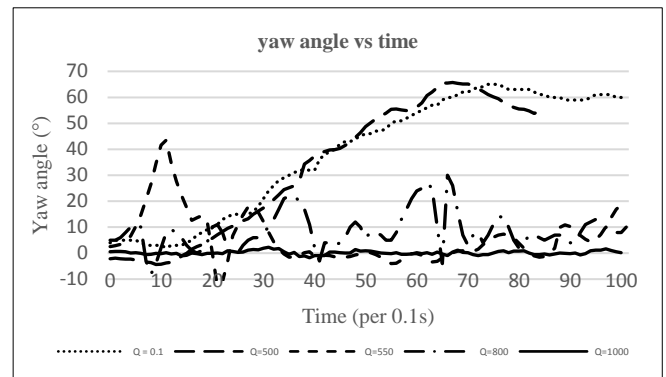


Figure 13. Graph of yaw angle versus time with variation of Q value

The best Q value to control yaw angle of quadrotor is 0.1. The oscillation will be held when the system is given the Q value less than 0.1. This happens because of the compass sensor is strongly influenced by magnetic field of electronic component. So, the situation will produce a fluctuating yaw angle which is used to the control yaw axis of quadrotor.

In the best Q value, quadrotor was able to maintain yaw angle in the angle range of 0° to 2° with a yaw angle obtained an average of $0,16^\circ$ and a standard deviation of 0.74° .

From all orientation angles test, LQR control can handle disturbance that occurred in system of quadrotor. The roll and pitch angle has an error or a deviation less than 2 % from maximal deviation axis (90 degrees) of quadrotor is equal 1,8 degrees, while yaw angle has an error or a deviation less than 4% from maximal deviation z-axis (360 degrees) of quadrotor is equal 14,4 degrees [8].

Characteristic response control

The response characteristics of the roll and pitch depicted in Figure 14 to Fig. 16.

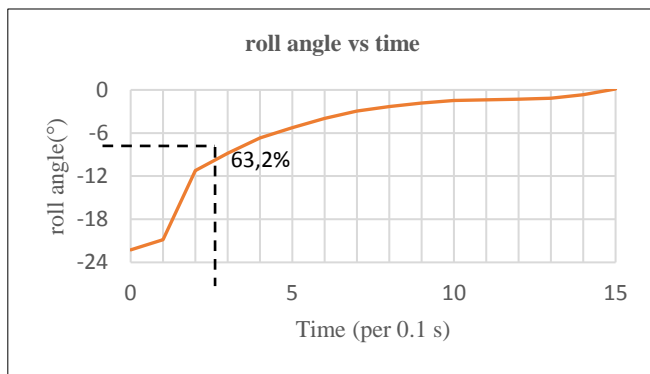


Figure 14 Characteristic response of roll angle

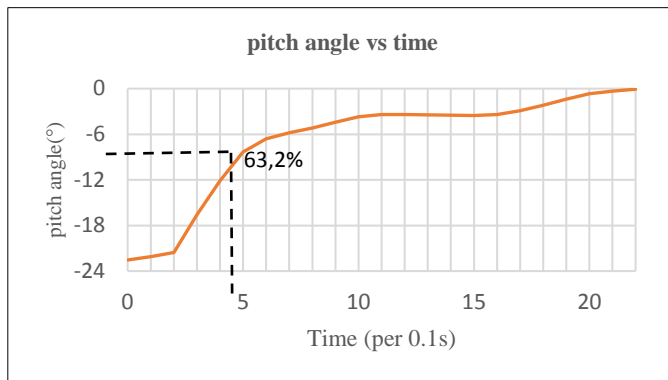


Figure 15 Characteristic response of pitch angle

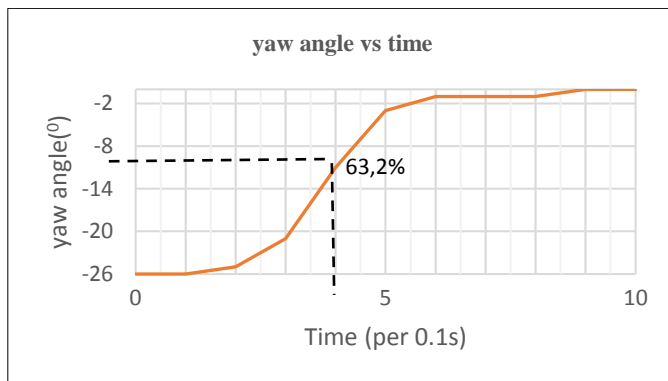


Figure 16 Characteristic response of yaw angle

The brushless motor of quadrotor is a system which has a first-order control system. The rise time of system can be determined by calculating time constant (τ_r). It can be obtained when the system reached 63.2% [7]. In other words, the orientation angle has reached 8.13° for the roll angle, 8.29° for the pitch angle and 9.57° for the yaw angle. In reaching that condition, from each corner takes time about 0.32×10^{-1} seconds for the roll angle, 0.52×10^{-1} seconds for the pitch angle and 0.42×10^{-1} , where the length of achievement time as the time constant of the system. Therefore, the fast response system or the rise time of the roll and pitch angle can be determined, τ_r towards roll angle is $(3,2 \times 10^{-2}) \ln 19 = 0,09$ seconds, τ_r towards pitch angle is $(5,2 \times 10^{-2}) \ln 19 = 0,15$ seconds and τ_r toward yaw angle is $(4,2 \times 10^{-2}) \ln 19 = 0,12$ seconds.

The response system of the three axes quadrotor been able to improve the system for less than 1 second. This happened due to a great disturbance from environmental factors when testing pitch angle [8]. However, with the rise time of this size on the roll and pitch angles, quadrotor is quickly able to overcome the disturbances and hovering very well.

VI. CONCLUSION

In this work, the control system using LQR methods has been implemented within experiment test in six state rotation of quadrotor. Based on experiment test results, the system responses represent the performance quadrotor in the hovering state has good stability in maintaining position of quadrotor. Quadrotor also products a very low steady state error. These results indicate that LQR controller makes quadrotor robustness.

In order further research, LQR methods will be combined using integrator concept, and implemented in 12 state model. So, the stability of quadrotor can be enhanced.

ACKNOWLEDGMENTS

Ministry of Research, Technology and Higher Education is acknowledged for Research Grant with contract number 156/LPPM/2015 and 781/UN1-P.III/LT.DIT-LIT/2016.

REFERENCE

- [1] T.K. Priyambodo, A.E. Putro, A. Dharmawan, "Optimizing Control based on Ant Colony for Quadrotor Stabilization", Jurnal of IEEE International Conference of ICARES, 2015.
- [2] G. Carrillo, et al., Quad Rotorcraft Control. London : Springer London, 2013,
- [3] H. Bolandi, et al., "Attitude Control of a Quadrotor with Optimized PID Controller", Intelligent Control and Automation, 2013, 4, pp. 335-342.
- [4] L.M. Argentin, et al., "PID, LQR and LQR-PID on a Quadcopter Platform", Informatics, Electronics & Vision, 2013 IEEE International Conference on, 2013.
- [5] M.R. Rahimi, S. Hajighasemi, D. Sanaei, "Designing and Simulation for Vertical Moving Control of UAV System using PID, LQR and Fuzzy logic", International Journal of Electrical and Computer Engineering, vol 3, no.5, pp.651-659, Oct 2013.
- [6] M.R. Rahimi, R. Ghasemi, D. Sanaei, "Designing Discrete Time Optimal Controller for Double inverted pendulum System", International Journal on Numerical and Analytical Methods in Engineering, 2013; 1(1): 3-7.
- [7] P. Corke, Robotics, Vision and Control, Berlin : Springer Berlin Heidelberg, 2011, pp. 78-80.
- [8] K. Ogata, Modern Control Engineering. Prentice Hall, 2010.
- [9] K. Nonami, et al., Autonomous Flying Robots. Japan: Springer Japan, 2010, pp. 2-7.
- [10] H. Chen, X. Wang, and Y. Li, "A Survey of Autonomous Control for UAV," in International Conference on Artificial Intelligence and Computational Intelligence, 2009, pp. 267-271
- [11] JMB. Domingues, Quadrotor Prototype, theses, Universidade Tecnica de Lisboa, 2009.
- [12] T. Bresciani, Modelling, Identification and Control of a Quadrotor Helicopter, 2008, pp 7-21.
- [13] SEAP. Costa, Controlo e simulação de um quadrirotor convencional, Master's thesis, october, 2008.
- [14] C. Balas, Modelling and Linear Control of a Quadrotor, M.Sc, theses, School of Engineering, Cranfield University, 2007.
- [15] Whidborne, J.F, 2007, Modelling And Linear Control Of A Quadcopter, Cranfield University.
- [16] S. Bouabdallah and R. Siegwart, "Back-Stepping and Sliding-Mode Techniques Applied to an Indoor Micro Quadrotor," Proceedings of the IEEE International Conference of Robotic and Automatic, 2005, pp. 2451-2456.
- [17] R. Prouty, Helicopter Performance, Stability, and Control. Krieger Publishing Company, 2002.

- [18] A. Chriette, Contribution à la commande et à la modélisation des hélicoptères, Phd Thesis, Université d'Evry, 2001.
- [19] R. Olfati-Saber, Nonlinear control of underactuated mechanical systems with application to robotics and aerospace vehicles, Phd thesis, MIT, 2001
- [20] S. Sastry, A mathematical introduction to robotic manipulation, Boca Raton, FL, 1994.